THE ASTROPHYSICAL JOURNAL, 336:593–600, 1989 January 15

ULTRA–HIGH-ENERGY PHOTONS FROM ACTIVE GALACTIC NUCLEI: THEORY

MAREK SIKORA AND ISAAC SHLOSMAN[1]
Joint Institute for Laboratory Astrophysics, University of Colorado and National Bureau of Standards
Received 1987 October 29; accepted 1988 June 26

ABSTRACT

First-order Fermi acceleration in collisionless shocks is supposed to operate in the central regions of active galactic nuclei (AGNs). Most of the shock energy is channeled into relativistic protons. Protons are effectively "cooled" as a result of interactions with the soft radiation produced by accreting matter. Among final products of such collisions are ultra–high-energy photons. For a certain range of parameters, we find that a substantial part of these photons leak out of the central region. They are absorbed by radio photons within 1 pc or escape much further, being uniformly absorbed within 10–30 kpc by the background microwave radiation. The above outcome depends upon the compactness of the central source. In both cases ultrarelativistic pairs are created. These pairs cool by means of synchrotron radiation in the interstellar magnetic field and form either compact hard γ-ray sources ($\sim 10^4$–10^6 MeV) or extended X-ray and γ-ray halos (0.01–100 MeV) around AGNs. Detection of such radiation would strongly support the hypothesis that proton-photon injection of ultrarelativistic pairs is responsible for nonthermal radiation from AGNs.

Subject headings: quasars — galaxies: nuclei — particle acceleration — radiation mechanisms

I. INTRODUCTION

As was proposed by Sikora *et al.* (1987, hereafter SKBS), relativistic electrons/positrons, responsible for nonthermal radiation of AGNs, can result from a pair cascade, initiated by injection of ultrarelativistic pairs by ultrarelativistic protons and supported by synchrotron radiation. It was shown by several authors that relativistic protons can be produced efficiently in collisionless shocks (Ellison and Eichler 1984; Blandford and Eichler 1987). They are cooled by interactions with cold matter, i.e., in proton-proton collisions (Protheroe and Kazanas 1983; Kazanas and Ellison 1986; Zdziarski 1986) and by interactions with soft radiation resulting in meson or electron-positron pair production (Blumenthal 1970; Colgate 1983; SKBS). For strong shocks, supposed to operate in the central regions of AGNs, SKBS have shown that the most efficient cooling mechanism of ultrarelativistic protons is photomeson production. Mesons decay into ultra–high-energy (UHE) photons ($>10^{14}$ eV), ultrarelativistic electrons/positrons, and neutrinos. The latter escape, while photons and e^+/e^- induce an electromagnetic pair cascade sustained by synchrotron radiation. Such a model avoids the difficulties of direct energy transfer from shocks to relativistic electrons.

In this paper we raise the possibility that the UHE photons in fact can leak out of the central region. We calculate the fraction of escaping photons and discuss their importance for our understanding of the ongoing physical processes in the galactic nuclei.

In the first place, the escaping photons can be absorbed by radio photons in the central radio source. The latter is related geometrically and probably physically to the broad emission line region (Preuss and Fosbury 1983). In the second place, the UHE photons can escape to the interstellar medium, provided that the AGN has a low radio emission compactness. They will be effectively absorbed by the microwave background radiation with a mean free path $\sim$10–30 kpc (e.g., Gould and Rephaeli 1978). In both cases the $\gamma\gamma$ absorption creates ultrarelativistic pairs which subsequently cool via synchrotron radiation. The spectral shape of the synchrotron radiation and its frequency range will depend upon the spectrum of the UHE radiation leaked out from the central source, as well as on the external magnetic fields. We show that the energy of this radiation will concentrate in the hard γ-rays if produced in the central radio source, and in the hard X-rays to mid-γ-rays if produced in the extended halo. The halo nonthermal radiation, when detected, can provide an independent estimate for the mass of the black hole in the AGN. We restrict ourselves to the theoretical aspects of the problem.

The outline of this paper is as follows: in § II we analyze the formation of UHE spectrum inside the central source. In § III we calculate the escape probability of the UHE photons, the energy spectra of created electron-positron pairs, and their synchrotron radiation in the external regions. Conclusions are presented in § IV.

II. PRODUCTION OF UHE PHOTONS BY RELATIVISTIC PROTONS IN ACTIVE GALACTIC NUCLEI

According to the recently developed theory of particle acceleration in collisionless shocks (see review by Blandford and Eichler 1987), relativistic protons are produced at a rate described well by a power-law function, $(\dot{N}_p)_{\gamma_p} \propto \gamma_p^{-\Gamma}$, with $\Gamma \lesssim 2$ for the compression ratio $\gtrsim 4$ (γ_p is a proton Lorentz factor). An upper limit on the proton energy follows either from the constraint on the proton acceleration time, which cannot exceed its cooling time, or from the comparison of the shock size to the proton gyroradius (whichever constraint gives the smaller γ_p). In the case of AGNs having dense soft radiation with the spectral index $\alpha_s < 1.2$, the cooling of the most relativistic protons is dominated by photomeson production of neutral pions, and the maximal proton energy is given by $t_{\rm acc} = t_{p\gamma}$ (see Fig. 2 of SKBS), where

$$t_{\rm acc} \propto r\alpha^{-2}\gamma_p B^{-1}$$

[1] Now at Theoretical Astrophysics, California Institute of Technology, Pasadena, California.

is the time scale of proton acceleration and

$$t_{p\gamma} \propto rM_{\rm BH}/l\gamma_p^{\alpha_s}(1+\tau/3)$$

is the time scale of proton cooling due to interaction with the soft radiation field. The parameters are $r = R(GM_{\rm BH}/c^2)^{-1/2}$, α is the accretion velocity/free-fall velocity, B is the magnetic field intensity at radius r, $M_{\rm BH}$ is the mass of the central black hole, $l = L\sigma_T/4\pi Rm_e c^3$ is the compactness parameter related to the nonthermal luminosity L of the AGN, and $\tau = \sigma_T N_e R$ is the optical thickness for Thomson scattering. Note that for the Eddington luminosity, i.e., $L = L_{\rm Edd}$, and $r = 10$, the compactness of the source is $l \simeq 200$.

Introducing the parameter $\epsilon_B = (B/B_{\rm eq})^2$, where $B_{\rm eq} = (8\pi GM_{\rm BH} m_p N_p/R)^{1/2}$ is the equipartition magnetic field, we obtain

$$\gamma_{p,\max} = 5.7 \times 10^8 \left[\frac{\alpha^3 \epsilon_B M_8}{\epsilon_{\rm rad} gl(1+\tau/3)^2 r^{3/2}}\right]^{1/4}, \quad (1)$$

where $\epsilon_{\rm rad} = L/\dot{M}c^2$ is the radiation efficiency, $M_8 = M_{\rm BH}/10^8 M_\odot$, and g is a geometrical factor describing departure from spherical accretion: $\dot{M} = 4\pi R^2 g N_p m_p v_{\rm in}$. Here $v_{\rm in}$ is the inflow (accretion) velocity. The spectral index of soft radiation, α_s has been taken equal to unity, as explained at the end of this section (see Appendix A for the numerical factor in $\gamma_{p,\max}$).

Since the time scale of proton cooling increases as the proton energy decreases, there is a certain value,

$$\gamma_{p,1} = 4.8 \times 10^7 \frac{\alpha}{lr^{1/2}(1+\tau/3)}, \quad (2)$$

below which the cooling time scale $t_{p\gamma}$ is longer than the accretion time scale (eq. [A1]), $t_{\rm in} \propto r^{3/2} M_{\rm BH}\alpha^{-1}$, and therefore production of mesons by protons with $\gamma_p < \gamma_{p,1}$ can be ignored (see Appendix A for the numerical factor in $\gamma_{p,1}$). The values of $\gamma_{p,\max}$ and $\gamma_{p,1}$, multiplied by a factor $K_\pi m_p/2m_e \simeq 240$ (where $K_\pi \simeq 0.26$ is an average fraction of proton energy transferred to mesons per interaction; Stecker 1968), determine the limits $x_{0,\max} \equiv h\nu_{0,\max}/m_e c^2$ and $x_{0,\min} \equiv h\nu_{0,\min}/m_e c^2$ of the UHE photon spectrum dominated by π^0 decay.[2] The spectral index of such photons is the same as for protons, so the UHE photon production rate is $\dot{n}_{x_0} \propto x_0^{-\Gamma}$, where $x_0 \sim 240\gamma_p$.

Most UHE photons are absorbed by the AGN's soft radiation, producing ultrarelativistic pairs. Since the cutoff of the soft radiation in AGNs, believed to result from self-synchrotron absorption, is in the far-infrared at $10^{-8} < x_{\rm abs} < 10^{-7}$ (Edelson 1987), electrons with $\gamma_e > x_{0,\min}$ cannot be cooled effectively by the Compton processes, since scattering occurs in the Klein-Nishina regime, i.e., $x_{\rm abs}\gamma_e > 1$. These electrons are cooled predominantly via synchrotron radiation. The synchrotron spectrum extends up to

$$x_{s,\max} \simeq x_B \gamma_{e,\max}^2 \simeq 1.5 \times 10^{11} \frac{1}{1+\tau/3} \frac{\alpha\epsilon_B}{\epsilon_{\rm rad} gr^{3/2}}, \quad (3)$$

[2] Photomeson production on relativistic protons is dominated by two branches of comparable cross sections, $p\gamma \to p\pi^0$ and $p\gamma \to n\pi^+$, followed by decays, $\pi^0 \to 2\gamma$ and $\pi^+ \to \mu^+\nu_\mu$, $\mu^+ \to e^+\nu_e\bar{\nu}_\mu$. Ultrarelativistic positrons produce UHE photons, but since three-fourths of the energy in the second branch is taken away by neutrinos, the first branch dominates as a source of such photons. For the neutrons, analogically, more UHE photons follow $n\gamma \to n\pi^0$ than $n\gamma \to p\pi^-$.

where $x_B = B/B_{\rm crit}$ and $B_{\rm crit} = m_e^2 c^2/\hbar c \simeq 4.4 \times 10^{13}$ G. This is much above the value

$$x_* \simeq 1.7 \times 10^2 \frac{1}{(1+\tau/3)l}, \quad (4)$$

at which the optical thickness for pair production $\tau_{\gamma\gamma} = 1$. Thus, most of the synchrotron radiation is absorbed and the next generation of pairs is produced. Since $x_B\gamma_{e,\max} \gtrsim 1$, the pair cascade proceeds through at least three generations of electrons and photons (Svensson 1987). As a result, the emerging spectrum can be approximated by one or two power-law branches with the spectral index α_s:

$$\alpha_s \simeq \begin{cases} 1 & \text{for Max } (x_c; x_{\rm abs}) < x < x_*, \\ 0.5 & \text{for } x_{\rm abs} < x < x_c, \quad \text{if } x_c > x_{\rm abs}, \end{cases} \quad (5)$$

where

$$x_c = (x_*^2/4)x_B = 2.3 \times 10^{-7}(\epsilon_B/\alpha g\epsilon_{\rm rad} M_8 l^3 r^{3/2})^{1/2}. \quad (6)$$

The flattening of the spectrum below x_c (if $x_c > x_{\rm abs}$) takes place because radiation is produced at these frequencies by pairs which have cooled from higher energies ($\gamma_e > x_*/2$), rather than by pairs directly injected by photons with $x < x_*$, at which $\tau_{\gamma\gamma}(x) < 1$.

Note that the UHE photons with energies $x_0 > 10^9$ interact mostly with photons having energies around $x_{\rm abs}$ (far-infrared). Thus, the break in the spectrum significantly decreases the absorption of the UHE photons if $x_c \gg x_{\rm abs}$. It will only insignificantly alter the proton cooling rate, since protons interact mostly with near-infrared and optical photons.

III. THE LEAKAGE OF UHE PHOTONS FROM ACTIVE GALACTIC NUCLEI

The spectrum of UHE photons leaking from the central source is

$$\dot{n}_{x_0}^{\rm esc} = \dot{\eta}_{x_0}\eta_{\rm esc}(x_0), \quad (7)$$

where $\eta_{\rm esc}(x_0)$ is the escape probability for a single photon with energy x_0. The escape probability of the photons depends upon their energy through the optical thickness for $\gamma\gamma$ pair production, $\tau_{\gamma\gamma}(x_0)$. Clearly $d\eta_{\rm esc}/d\tau_{\gamma\gamma} < 0$. Since $x_0 > 240\gamma_{p,1} > 1/x_{\rm abs}$, we have $d\tau_{\gamma\gamma}(x_0)/dx_0 < 0$. Thus, the leaked UHE photon spectrum is flatter than the primary one, and its energy peaks strongly around $x_{0,\max} \approx 240\gamma_{p,\max}$. To specify the functions $\tau_{\gamma\gamma}(x_0)$ and $\eta_{\rm esc}(\tau_{\gamma\gamma})$, the volume distributions of the far-IR and the UHE photon emission must be known. In our calculations we have adopted (for $\tau_{\gamma\gamma} \gg 1$)

$$\eta_{\rm esc}(x_0) = \frac{1-\exp[-\tau_{\gamma\gamma}(x_0)]}{\tau_{\gamma\gamma}(x_0)} \simeq \frac{1}{\tau_{\gamma\gamma}(x_0)}, \quad (8)$$

which approximates the idealized case, when both photon populations are uniformly produced over the volume. The UHE photons, hence, are assumed to be uniformly and isotropically distributed in the center and have a radial (anisotropic) distribution outside. In calculations of $\tau_{\gamma\gamma}(x_0)$ we have included an optically thin part of the soft photon spectrum $n_x \propto x^{-(\alpha_s+1)}$, as well as its thick part, $n_x \propto x^{3/2}$ (for $x < x_{\rm abs}$). In Figure 1 we demonstrate the dependence of the escape probability, $\eta_{\rm esc}$, on the UHE photon energy, x_0, parameterized by the mass of the central black hole, $M_{\rm BH}$, and by the compactness parameter, l. The relations presumed there can be roughly approximated by equation (B8).

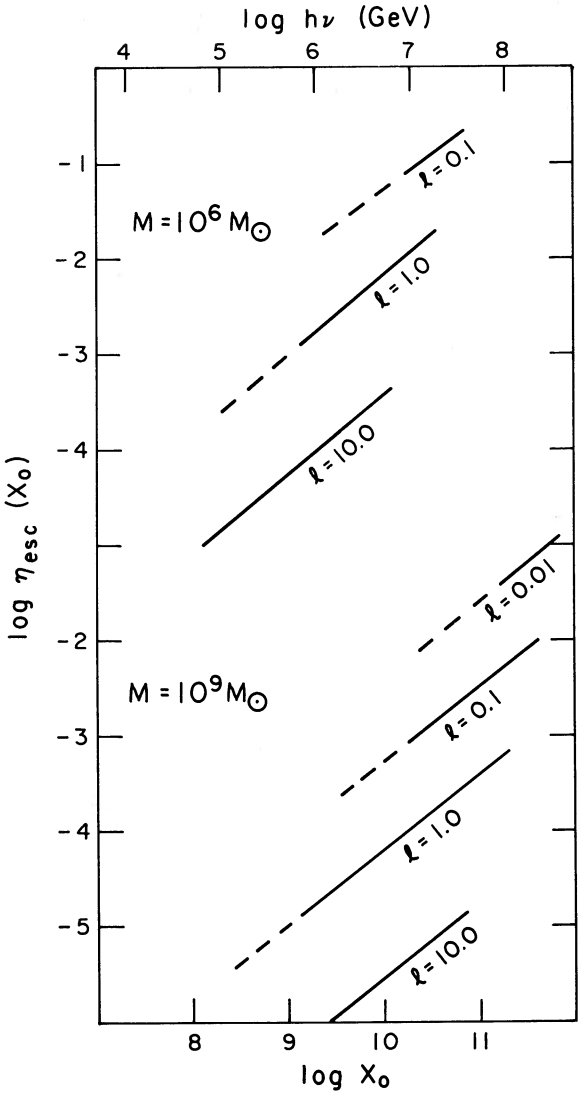

FIG. 1.—Escape probability for the UHE photons as a function of their energy x_0, for $M_{BH} = 10^6$ and 10^9 $M_\odot$, and for different values of the compactness parameter l. Other parameters have been fixed at $\epsilon_B = 1$, $\epsilon_{rad} = 0.01$, $\alpha = 0.5$, $g = 0.5$, $r = 10$, and $\Gamma = 1.5$.

Depending on the compactness of the central radio source, the escaping UHE photons can be absorbed inside $R \sim 1$ pc by the radio photons or can penetrate the interstellar region. In the latter case, they can propagate up to the distances of ~10–30 kpc, determined by the mean free path of the UHE photons in the background microwave radiation (Gould and Rephaeli 1978 and references therein). The radio source is transparent at a frequency ν for a UHE photon, if

$$\tau_{\gamma\gamma}\left(x_0 = \frac{m_e c^2}{h\nu}\right) \sim 44.5\left(\frac{L_\nu}{10^{30}\ \mathrm{ergs\ s^{-1}\ Hz^{-1}}}\right)\left(\frac{R}{1\ \mathrm{pc}}\right)^{-1} < 1 . \quad (9)$$

There are AGNs for which condition (9) is violated (e.g., Pearson and Readhead 1983; Preuss and Foxbury 1983). However, on the basis of the present data we cannot rule out the possibility that some AGNs (maybe the majority) have radio sources too weak or too diffuse to absorb the UHE photons (Condon *et al.* 1981; Unger *et al.* 1986; Condon, Gower, and Hutchings 1987). Both cases are considered below.

a) $\tau_{\gamma\gamma} \ll 1$ *in the Radio Source*

Let us approximate the probability of absorption of the UHE photon in the background microwave field at a distance R by $\sim R/R_{max}(x_0)$, where $R_{max}(x_0)$ is equal to the mean free path of the UHE photons in the background radiation. The absorption rate of the UHE photons in the shell of thickness ΔR located at distance R from the central source is given then by

$$\dot{n}^{abs}_{x_0}(R) 4\pi R^2\, dR \simeq \frac{L^{esc}_{x_0}}{x_0 m_e c^2}\frac{\Delta R}{R_{max}(x_0)} . \quad (10)$$

$R_{max}(x_0)$ is shown in Figure 2 for the present epoch and depends solely on the energy density of the background photons.

The spectrum of created electrons/positrons is roughly equal to $\dot{N}_{\gamma_e}(R) = 4\dot{n}^{abs}_{x_0}(R)$, where $\gamma_e = x_0/2$. We neglect the asymmetry between the energies of created particles, since it cannot alter our results by a factor larger than 2. Assuming equal energies drastically simplifies the calculations. The pairs are cooled by Compton interactions with background photons or by synchrotron radiation in the interstellar magnetic fields. If the intensity of the magnetic field is $B_{ISM} > 0.1$ μG, synchrotron cooling is more efficient (Protheroe 1986), and this case is considered by us hereafter (note the change of notation for interstellar magnetic field and $x_{B,\,ISM}$). The amount of synchrotron radiation emitted per unit frequency and per unit volume is

$$\dot{u}^{syn}_x(R)dx \simeq \dot{\gamma}_e m_e c^2 N_{\gamma_e} d\gamma_e , \quad (11)$$

where x is the dimensionless frequency of the synchrotron photon, which is related to the electron energy as $x \simeq \gamma_e^2 x_{B,ISM}$, and $\dot{\gamma}_e$ is the rate of electron cooling. For the steady state electron flow in the energy space we have

$$N_{\gamma_e}\dot{\gamma}_e = \int_{\mathrm{Max}\,(\gamma_e;\,\gamma_{e,1})}^{\gamma_{e,\max}} \dot{N}_{\gamma_e} d\gamma_e , \quad (12)$$

where $\gamma_{e,1} = x_{0,min}/2$ and $\gamma_{e,max} = x_{0,max}/2$. Finally, combining equations (11) and (12), we get the spectrum of synchrotron radiation emitted in the dR shell:

$$\frac{dL^{syn}_x}{dR} = 4\pi R^2 \dot{n}^{syn}_x(R)$$
$$= \frac{2\pi R^2 m_e c^2}{(x x_{B,ISM})^{1/2}} \int_{\mathrm{Max}\,(\gamma_e;\,\gamma_{e,1})}^{\gamma_{e,\max}} \dot{N}_{\gamma_e}(R) d\gamma_e \quad (13)$$
$$= \frac{L_0}{I_0}\frac{1}{(x x_{B,ISM})^{1/2}} \int_{\mathrm{Max}\,(x_{0,min};\,x_0)}^{x_{0,\max}} \frac{\eta_{esc}(x_0) x_0^{-\Gamma} dx_0}{R_{max}(x_0)} ,$$

where L_0 is the total luminosity of the UHE radiation produced inside the central source, $x_0 = 2(x/x_{B,\,ISM})^{1/2}$ and

$$I_0 = \int_{x_{0,\,min}}^{x_{0,\,max}} x_0^{1-\Gamma} dx_0 . \quad (14)$$

Note that because most of the UHE photons are reprocessed just in the central source, L_0 is equal to the luminosity L of the nonthermal component of AGNs.

The synchrotron spectra produced in halo shells of thickness $\Delta R = 1$ kpc at any distance $R <$ Min $[R_{max}(x_0)]$ are shown for

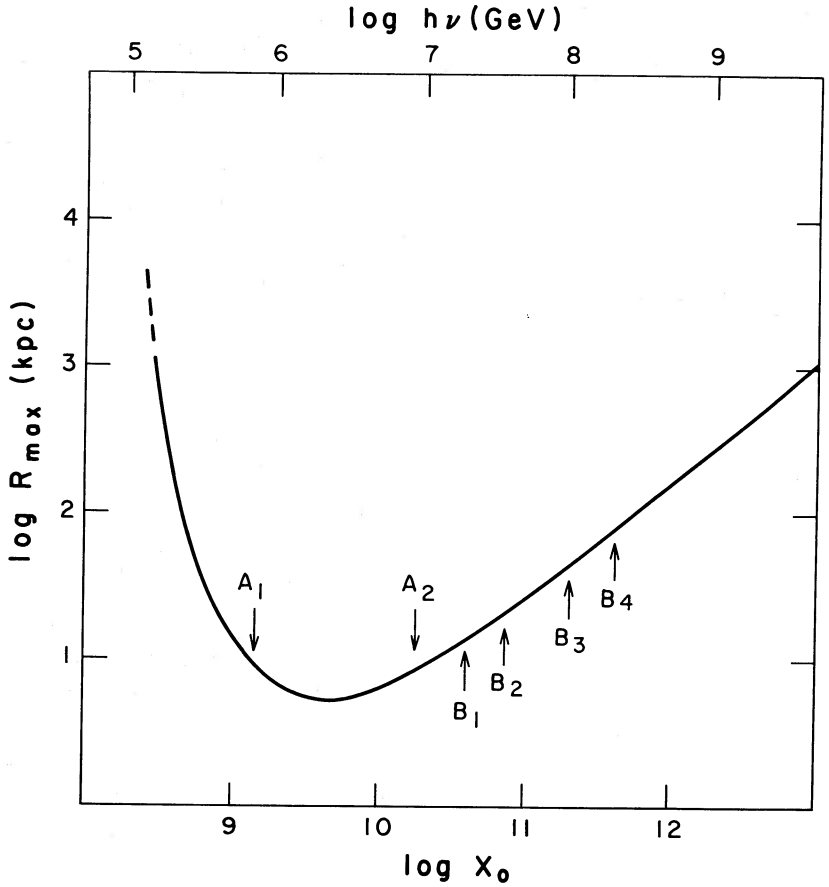

FIG. 2.—Mean free path of the UHE photons interacting with the microwave background radiation, as a function of their energy x_0. In addition, the range of the emerging spectrum of the UHE radiation is shown: A_1B_1 (for $10^6\ M_\odot$, $l = 1$), A_2B_2 (for $10^6\ M_\odot$, $l = 0.1$), A_1B_3 (for $10^9\ M_\odot$, $l = 1$), and A_2B_4 (for $10^9\ M_\odot$, $l = 0.1$). Other parameters are as in Fig. 1.

a set of parameters on Figure 3. Clearly these spectra peak close to the high-energy cutoffs. The spectrum shapes for the cases $x_{0,\,\min} < x_0 \ll x_{0,\max}$ can be calculated from equation (13) using the approximate relations $\eta_{\rm esc}(x_0) \simeq \tau_{\gamma\gamma}^{-1}(x_0) \propto x_0^{1-\Delta_1}$ and $R_{\max}(x_0) \propto x_0^{1-\Delta_2}$, where $0 \lesssim \Delta_1 < 1$ (see eq. [B4]) and $0 < \Delta_2 < 1$ for $x_0 > 10^{10}$ (see Fig. 2). Hence we obtain, using $x_0 \propto x^{1/2}$,

$$F_x x \propto x^{1-\Gamma/2+(\Delta_2-\Delta_1)/2}\ . \tag{15}$$

Therefore, for $\Gamma < 2$ and $(\Delta_2 - \Delta_1)/2 < 1$, $F_x x$ has a maximum value close to the high-energy limit.

In all cases for $x < x_1$, where $x_1 = x_{0,\min} x_{B,\rm ISM}/4$, the spectrum $F_x x$ is proportional to $x^{1/2}$, since it is produced only by electrons cooled to the corresponding energies $[\gamma_e \sim (x/x_{B,\,\rm ISM})^{1/2}]$ without direct injection of electrons with such energies.

In Figure 4 we demonstrate the halo spectra, $F_{x,\,\rm tot}\, x$, integrated over the radius R. Most of the nonthermal energy is radiated in the 0.1–100 MeV band for black hole masses $\sim 10^6$–$10^{10}\ M_\odot$ and $B_{\rm ISM} \sim 1\ \mu$G, characteristic of large-scale galactic magnetic field (e.g., Asseo and Sol 1987) and references therein).

The total luminosity of the halo synchrotron radiation is given by $L_{\rm esc} = \xi_{\rm esc} L_0$, where $\xi_{\rm esc}$ is the efficiency of escape for the UHE radiation, namely,

$$\xi_{\rm esc} = \frac{\int_{x_{0,\min}}^{x_{0,\max}} dx_0\, x_0^{1-\Gamma} \eta_{\rm esc}(x_0)}{\int_{x_{0,\min}}^{x_{0,\max}} dx_0\, x_0^{1-\Gamma}}\ . \tag{16a}$$

Using the approximation for $\tau_{\gamma\gamma}(x_0)$ and $\eta_{\rm esc}(x_0)$ given by equation (B8) will yield

$$\xi_{\rm esc} \propto \begin{cases} l^{-1/2-\Delta_1} M_8^{-1/2} & \text{for } x_c < x_{\rm abs}\ , \\ l^{-1-\Delta_1} M_8^{-1/2} & \text{for } x_c > x_{\rm abs}\ . \end{cases} \tag{16b}$$

In Figure 5 we superpose the lines of constant $\xi_{\rm esc}$ on the curves of total halo luminosity, $L_{\rm esc}$, versus L_0, for different $M_{\rm BH}$ and l.

b) $\tau_{\gamma\gamma} > 1$ *in the Radio Source*

This case is more uncertain for the numerical treatment than case *a*, because we do not know the spatial distribution and the spectrum of the radiation absorber, which is now the radio source. Nevertheless, if we assume that the magnetic field $B_{\rm rs}$ is approximately constant over the entire volume of the radio source with the radius $R_{\rm rs}$, it is possible to avoid these uncertainties, computing the spectrum of the synchrotron radiation from the whole region at once. By modifying equations (11) and (12), applying them to the $\gamma\gamma$ absorption region as a whole, and replacing $x_{B,\rm ISM}$ by $x_{B,\rm rs} = B_{\rm rs}/B_{\rm crit}$, we obtain

$$L_x^{\rm syn} = \frac{L_0}{I_0} \frac{1}{(x x_{B,\rm rs})^{1/2}} \int_{\rm Max\,(x_0,\min;\, x_0)}^{x_{0,\max}} \eta_{\rm esc}(x_0) x_0^{-\Gamma}\, dx_0\ , \tag{17}$$

where $x_0 = 2(x/x_{B,\rm rs})^{1/2}$. Since the function $\eta_{\rm esc}(x_0) x_0^{-\Gamma}$ is very flat, $\sim x_0^{1-\Gamma}$, the resulting $L_x^{\rm syn}$ is well approximated by the

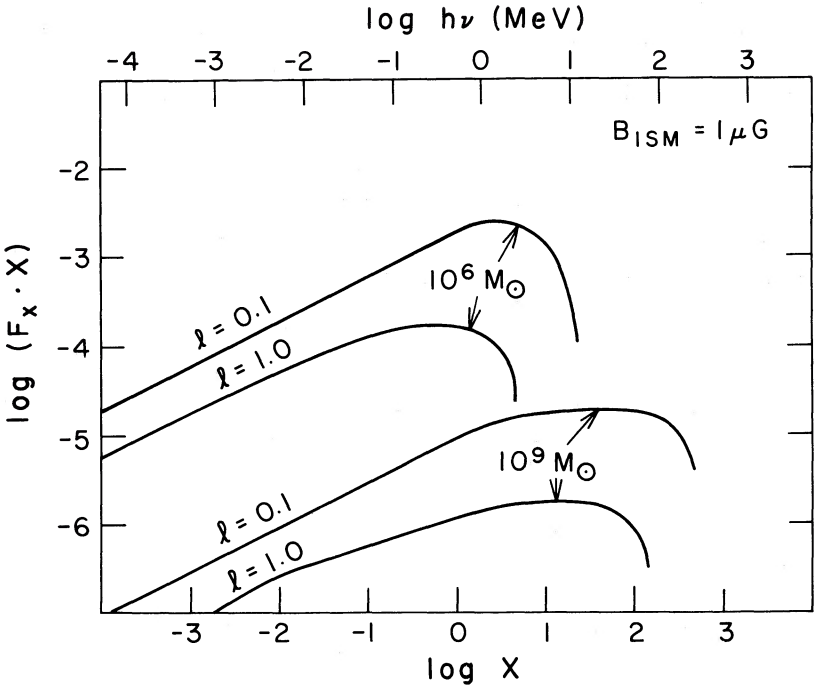

FIG. 3.—Synchrotron spectra of AGN halo shells with thickness $\Delta R = 1$ kpc, for different M_{BH} and l, in units of ergs s^{-1}. The interstellar magnetic field is $B_{ISM} = 1$ μG. Other parameters are as in Fig. 1.

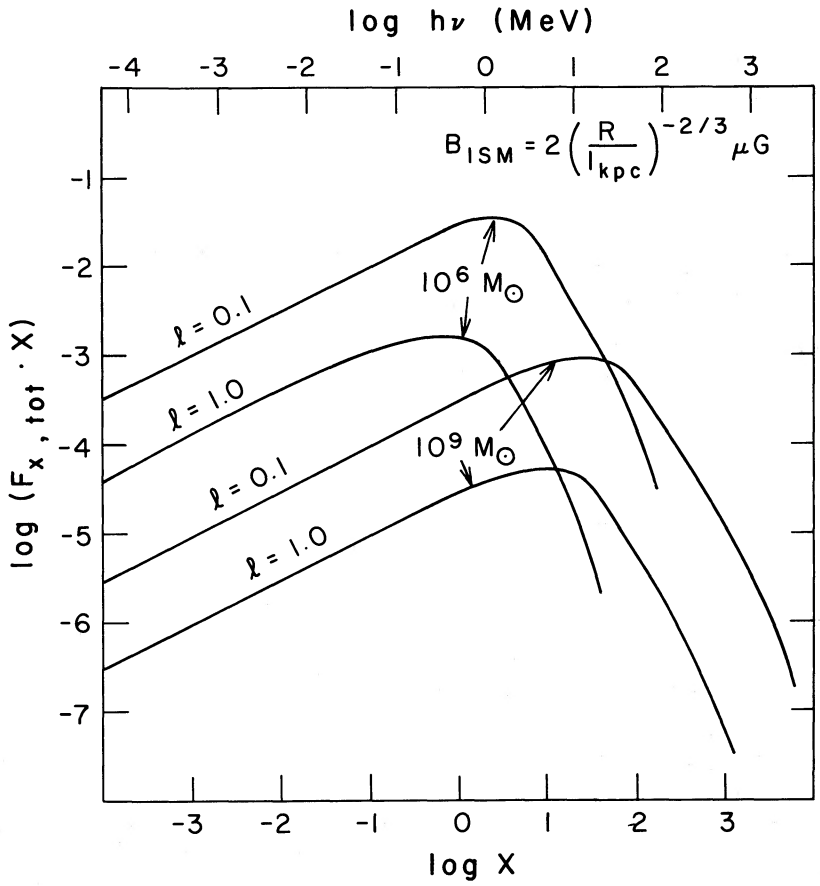

FIG. 4.—Integrated (over R) synchrotron spectra of the AGN halo for different M_{BH} and l, in units of ergs s^{-1}. The interstellar magnetic field is $B_{ISM} \simeq 2(R/1\ \mathrm{kpc})^{-2/3}$ μG. Other parameters are as in Fig. 1.

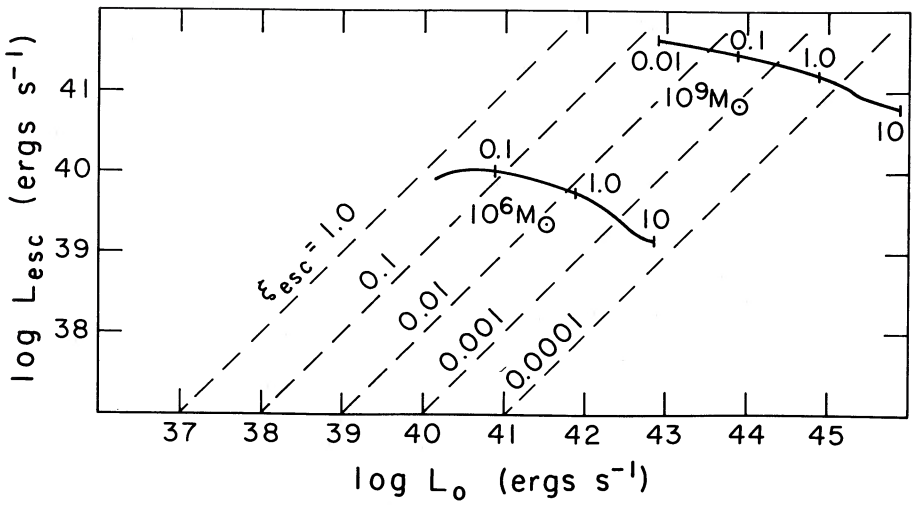

FIG. 5.—Total halo luminosity vs. nonthermal AGN luminosity for different M_{BH} and l. Also shown are the lines of constant efficiency for escaping UHE radiation. Other parameters are as in Fig. 1.

power law with slope $\beta = 0.5$ up to $x \sim x_{max}$ and by the cutoff above it. So, energetically the spectrum peaks around x_{max}, which is now B_{rs}/B_{ISM} times larger than in case *a*. If the magnetic and thermal energy densities are comparable in the broad emission line region of the AGN, the magnetic field is $B_{rs} \sim 0.01$ G and the resulting spectra peak at $h\nu_{max} \sim 10^4$–10^6 MeV for the black hole masses $\sim 10^6$–10^{10} $M_\odot$. The shape of the high-energy cutoff in the spectrum depends upon the magnetic field distribution. The cutoff will have an extended high-energy tail composed of maxima produced at different radii. Using the same arguments, the total halo synchrotron spectra (Fig. 4) will have the high-energy tails, while the dR shells will have the sharp cutoffs (Fig. 3). However, if $x_{max} > x_1 = 100\ (R_{rs}/R_{cen})/(1 + \tau/3)l$, where R_{cen} is the size of the central region, then the pair cascade must be involved. The latter is caused by absorption of hard γ-rays by the IR-optical photons from the central source and sustained by Compton process on these photons. It provides reshaping of the synchrotron spectrum and shifts x_{max} down to x_1, at which $\tau_{\gamma\gamma} = 1$.

Recently Rees (1987) proposed that the magnetic fields in the broad emission line regions of AGNs can be as high as ~ 1 G, being responsible for the confinement of the emission-line clouds. Then $h\nu_{max} \sim 10^8$ MeV, and the energetically dominant fraction of the synchrotron radiation, at $x_1 < x < 10^8$, is absorbed by the IR photons which are produced locally or centrally. As a result, the next generation of pairs will emerge and cool mainly through a synchrotron mechanism, because now $B^2/8\pi > L_{IR}/4\pi R^2 c$. The resulting spectrum cuts off at $h\nu < 10^2$ MeV, where it cannot compete with the radiation from the central source. Thus, for $B \sim 1$ G, the high-energy spectrum, around x_1, produced in the ~ 1 pc region is determined by the first generation of the synchrotron radiation, which is cut off at x_1 and has luminosity reduced by a factor $\sim (x_{max}/x_1)^{1/2}$. Hence, the lower B_{rs}, the higher are the luminosities of the compact 10^4–10^6 MeV γ-ray source predicted by our model.

IV. DISCUSSION

We have investigated the formation and escape of UHE photons in AGNs. Most of the UHE radiation is absorbed on the spot and supports the pair cascade inside the central source, but approximately $\sim 10^{39}$–10^{42} ergs s^{-1} leak out. These UHE photons are absorbed either by the radio photons inside $R \sim 1$ pc, or by the background microwave radiation within ~ 30 kpc, the outcome depending on the compactness of the central radio source. In both cases the $\gamma\gamma$ absorption results in creation of the ultrarelativistic pairs which cool via synchrotron radiation. The efficiency of escape depends on two parameters—the mass of the black hole and the compactness of the source, approximately as

$$\xi_{esc} \simeq 1.5 \times 10^{-2} (l/0.1)^{-1.2} M_8^{-0.5} . \quad (18)$$

This estimate of ξ_{esc} follows from relations (16a) and (16b) and is valid for $x_c > x_{abs}$, when the flattening of the spectrum of synchrotron radiation in AGNs takes place (see § II). The value of $\Delta_1 = 0.2$ has been fixed, to provide a close match with Figure 5, for the range of $M_{BH} \simeq 10^6$–10^{10} $M_\odot$ and $l \simeq 10^{-2}$–10.

When the absorption in the central radio source is negligible, the escaping UHE photons from AGNs interact with the microwave background radiation and produce pairs. The mean free path of UHE photons, $R_{max}(x_0)$, has been calculated and is shown in Figure 2. It is independent of M_{BH}. Pairs in the interstellar magnetic field produce a synchrotron halo. This radiation has a flat spectrum ($\beta \sim 0.5$, $F_\nu \sim \nu^{-\beta}$) extending up to

$$x_{max} \sim 10^2 l^{-1/2} M_8^{1/2} (B_{ISM}/1\ \mu G) , \quad (19)$$

as can be seen in Figures 3 and 4.

The measurement of the halo luminosity, L_{esc}, provides a possibility of observational determination of M_{BH}. If both L_{esc} and the nonthermal luminosity L of the AGN are known, Figure 5 can then be used trivially, as a precalculated map, to recover the compactness l and the mass M_{BH}. There are, however, technical constraints which must be overcome. First, to measure the halo nonthermal luminosity, it is necessary to have instrumental resolution corresponding to <5 kpc, in order to extract the much more luminous central source. The instrumental angular resolution must be then $\delta \sim (z/0.01)^{-1}$ arcminutes, where z is the cosmological redshift. Second, the absolute luminosity of the halo is quite low, $L_{esc} \sim 10^{41} M_8^{1/2}$

ergs s^{-1}, and hence a high sensitivity is required to detect the distant AGNs.

For the objects where most of the UHE photons are absorbed in the central radio source, the compact hard γ-ray source is formed with the energy output that is peaked at $\sim 10^4$–10^6 MeV. Direct photons produced in this energy range by the central region suffer strong absorption from the optical and IR photons. Their emerging luminosity cannot compete with the secondary γ-rays resulting from the absorption of the primary UHE photons in the radio source. Are the $\sim 3 \times 10^5$ MeV γ-rays detected in Cen A (Grindlay *et al.* 1975) produced this way? Future γ-ray telescopes should not have any difficulties detecting $\sim 10^{41}$ ergs s^{-1} at $\gtrsim 10^4$ MeV from the nearby AGNs.

Most of the AGNs are not listed in the radio catalogs and are called "radio-quiet." However, more sensitive surveys show that probably all AGNs have some central radio components (Condon *et al.* 1981; Unger *et al.* 1986). No data are presently available to estimate whether they are compact enough to block the UHE radiation from escaping. It is, therefore, plausible that X- and γ-ray nonthermal halos exist around AGNs, as our model predicts.

Detection of compact hard γ-ray sources with $h\nu > 10^4$ MeV or X- and γ-ray halos around AGNs would provide a strong argument in favor of efficient proton acceleration and of proton-photon injection of ultrarelativistic pairs, responsible for the formation of nonthermal continua in AGNs.

Finally, we emphasize that quantitative results presented in this paper should be taken with caution, mostly because of the very simplified treatment of the escape probability. We have ignored the self-consistent approach to the γ-ray transfer problem, omitting the transit zone, where the radiation field becomes anisotropic. Since most of the UHE photons which escape are formed in this surface layer, the actual escape probability can be affected strongly by the anisotropy and the inhomogeneity in this zone. We would like to note here a very interesting case which was not considered by us because of its sensitivity to the conditions in the transit region, but which can provide higher escape efficiencies. If shocks are *not* distributed uniformly over the central volume but rather are distributed arounds its outer edge, the absorption of the UHE photons will be sharply reduced.

Another omitted factor which can alter our results, but now in their "negative direction," is the magnetophoton opacity, i.e., opacity for pair creation due to photon interaction with virtual quanta of the magnetic field (e.g., Erber 1966). As a result of this process photons with $x \gtrsim 1/x_B$ are effectively absorbed. Because of the pair cascade operating in the transit zone, the energy of the photons with $x > x_B^{-1}$ is transferred to the photons with $x \lesssim x_B$, and a fraction of it, determined by the $\gamma\gamma$ absorption, will escape. The magnetophoton opacity would have its greatest effect on the low-mass Galactic compact sources, such as Cygnus X-3, where it would completely block all the UHE photons in the source. The low-mass sources have been excluded from our analysis for this reason.

We would like to thank the anonymous referee for pointing out the importance of the central radio sources in AGNs. We thank John Stocke for his helpful remarks and suggestions, and Mitch Begelman and Mike Shull for carefully reading and correcting this manuscript. The authors acknowledge support under the National Aeronautics and Space Administration Astrophysical Theory Center grant NAGW-766 and the National Science Foundation grant 83-51997.

APPENDIX A

RELEVANT TIMES SCALES

The time scales expressed as functions of parameters $\epsilon_{\rm rad}$, ϵ_B, g, α, r, l, and M_8 defined in the text are given below.

Accretion time scale onto the central black hole:

$$t_{\rm in} \simeq 5 \times 10^2 \frac{r^{3/2} M_8}{\alpha} \text{ s}; \tag{A1}$$

Proton acceleration time scale in a collisionless shock:

$$t_{\rm acc} \simeq 7.3 \times 10^{-8} \left(\frac{\epsilon_{\rm rad} g M_8 r^{7/2}}{\alpha^3 \epsilon_B l} \right) \gamma_p \text{ s}, \tag{A2}$$

Proton cooling time scale due to interaction with a soft radiation field with spectral index $\alpha_s \sim 1$:

$$t_{p\gamma} \simeq 2.4 \times 10^{10} \frac{r M_8}{(1 + \tau/3) l \gamma_p} \text{ s}. \tag{A3}$$

From $t_{\rm acc} = t_{p\gamma}$ we obtain the numerical factor 5.7×10^8 in the formula for $\gamma_{p,\max}$ (eq. [1]), and from $t_{\rm in} = t_{p\gamma}$ we obtain the numerical factor 4.8×10^7 in the formula for $\gamma_{p,1}$ (eq. [2]).

APPENDIX B

OPTICAL THICKNESS FOR PHOTON-PHOTON PAIR CREATION

The optical depth for photon-photon pair creation is calculated according to

$$\tau_{\gamma\gamma}(x_0) = \frac{4R}{x_0^2}\int_{1/x_0}^{\infty}\frac{n_x}{x^2}\,dx\int_1^{\sqrt{x_0 x}}\sigma_{\gamma\gamma}(x')x'^3\,dx' \tag{B1}$$

$$= \frac{4R}{x_0^2}\int_1^{\infty}\sigma_{\gamma\gamma}(x')x'^3\,dx'\int_{x'^2/x_0}^{\infty}\frac{n_x}{x^2}\,dx\,. \tag{B2}$$

For the power-law photon spectrum we write $n_x = C_s x^{-1-\alpha}$ and

$$\tau_{\gamma\gamma}(x_0) = \frac{4(C_s R\sigma_T)x_0^{\alpha}}{(2+\alpha_s)}\int_1^{\infty}\frac{\sigma_{\gamma\gamma}(x')}{\sigma_T}\,x'^{-(1+2\alpha)}\,dx'\,. \tag{B3}$$

For the photon spectrum,

$$n_x = \begin{cases} C_s x_{\rm abs}^{-7/2}x^{3/2} & \text{for } x < x_{\rm abs}\,, \\ C_s x^{-2} & \text{for } x > x_{\rm abs}\,, \end{cases}$$

and $x_0 \gg 1/x_{\rm abs}$, the optical thickness $\tau_{\gamma\gamma}(x_0)$ is found by us to be well approximated by

$$\tau_{\gamma\gamma}(x_0) \simeq \frac{(1+\tau/3)C_l}{x_0 x_a^2}\left[\frac{7}{8}\ln(x_0 x_{\rm abs}) - 0.7\right], \tag{B4}$$

where $C_l = C_s R\sigma_T/(1+\tau/3)$. Formula (B4) was obtained from equation (B3), using the asymptotic form of $\sigma_{\gamma\gamma}(x')$ for $x' \gg 1$:

$$\sigma_{\gamma\gamma}(x') \approx \frac{3}{8}\,\sigma_T\,\frac{1}{x'^2}\,[\ln(4x'^2) - 1]\,. \tag{B5}$$

If x_c, defined by equation (6), is greater than $x_{\rm abs}$, then the spectrum changes slope from $\alpha = 1$ at $x > x_c$ to $\alpha = 0.5$ at $x < x_c$. For this case we obtain

$$\tau_{\gamma\gamma}(x_0) \simeq \frac{(1+\tau/3)C_l'}{x_0 x_{\rm abs}'^{1.5}}\,[\ln(x_0 x_{\rm abs}') - 0.6]\,, \tag{B6}$$

where $x_{\rm abs}' = x_{\rm abs}(x_{\rm abs}/x_c)^{1/6}$ and $C_l' = C_l/x_c^{1/2}$.

In our parameterization the frequency $x_{\rm abs}$, at which the optical thickness for self-synchrotron absorption equals unity, is

$$x_{\rm abs} = 6.4\times10^{-8}(3+\Gamma)^{2/7}\left(\frac{\epsilon_B}{g\alpha\epsilon_{\rm rad}}\right)^{1/14}\frac{1}{r^{11/28}}\left(\frac{l}{M^8}\right)^{5/14} \tag{B7}$$

for $\alpha = 1$.

Since $C_l \propto l$, we get an approximate dependence of the photon escape probability, $\eta_{\rm esc}$, on x_0, M_B, and l:

$$\eta_{\rm esc}(x_0, l, M_{\rm BH}) \simeq \tau_{\gamma\gamma}^{-1}(x_0) \propto x_0 x_{\rm abs}^2/l \propto \begin{cases} x_0 l^{-2/7}M_8^{-5/7} & \text{for } x_c < x_{\rm abs}\,, \\ x_0 l^{-3/4}M_8^{-3/4} & \text{for } x_c > x_{\rm abs}\,, \end{cases} \tag{B8}$$

when $\tau_{\gamma\gamma} \gg 1$.

REFERENCES

Asseo, E., and Sol, H. 1987, *Phys. Rept.*, **148**, 307.
Blandford, R. D., and Eichler, D. 1987, *Phys. Rept.*, **154**, 175.
Blumenthal, G. R. 1970, *Phys. Rev. D*, **1**, 1596.
Colgate, S. A. 1983, *Proc. 18th Internat. Cosmic Ray Conf.*, **2**, 230.
Condon, J. J., Gower, A. C., and Hutchings, J. B. 1987, *A.J.*, **92**, 255.
Condon, J. J., O'Dell, S. L., Puschell, J. J., and Stein, W. A. 1981, *Ap. J.*, **246**, 624.
Edelson, R. 1987, Ph.D. thesis, California Institute of Technology.
Ellison, D. C., and Eichler, D. 1984, *Ap. J.*, **286**, 694.
Erber, T. 1966, *Rev. Mod. Phys.*, **38**, 626.
Gould, R. J., and Rephaeli, Y. 1978, *Ap. J.*, **225**, 318.
Grindlay, J. E., Helmken, H. F., Brown, R. H., Davis, J., and Allen, L. R. 1975, *Ap. J. (Letters)*, **197**, L9.
Kazanas, D., and Ellison, D. C. 1986, *Nature*, **319**, 380.
Pearson, T. J., and Readhead, A. C. S. 1983, in *IAU Symposium 110, VLBI and Compact Radio Sources*, ed. R. Fanti, K. Kellermann, and G. Setti (Dordrecht: Reidel), p. 15.
Preuss, E., and Fosbury, R. A. E. 1983, *M.N.R.A.S.*, **204**, 783.
Protheroe, R. J. 1986, *M.N.R.A.S.*, **221**, 769.
Protheroe, R. J., and Kazanas, D. 1983, *Ap. J.*, **265**, 620.
Rees, M. J. 1987, *M.N.R.A.S.*, **228**, 47P.
Sikora, M., Kirk, J. G., Begelman, M. C., and Schneider, P. 1987, *Ap. J. (Letters)*, **320**, L81 (SKBS).
Stecker, F. W. 1968, *Phys. Rev. Letters*, **21**, 1016.
Svensson, R. 1987, *M.N.R.A.S.*, **227**, 403.
Unger, S. W., Pedlar, A., Booler, R. V., and Harrison, B. A. 1986, *M.N.R.A.S.*, **219**, 387.
Zdziarski, A. A. 1986, *Ap. J.*, **305**, 45.

ISAAC SHLOSMAN: Theoretical Astrophysics, 130–33, California Institute of Technology, Pasadena, CA 91125

MAREK SIKORA: Nicolaus Copernicus Astronomical Center, Polish Academy of Sciences, Bartycka 18, 00-716 Warszawa, Poland